Biometric iris image acquisition system with wavefront coding technology

Sheng-Hsun Hsieh[a], Hsi-Wen Yang[a], Shao-Hung Huang[a], Yung-Hui Li[b] and Chung-Hao Tien[a]

[a]Dep. of Photonics, National Chiao Tung Univ./1001 University Rd., Hsinchu Taiwan 300, R.O.C.
[b]Dept. of Information Engineering and Computer Science, Feng Chia Univ./100 Wenhwa Rd., Seatwen, Taichung Taiwan 407, R.O.C.

Abstract

Biometric signatures for identity recognition have been practiced for centuries. Basically, the personal attributes used for a biometric identification system can be classified into two areas: one is based on physiological attributes, such as DNA, facial features, retinal vasculature, fingerprint, hand geometry, iris texture and so on; the other scenario is dependent on the individual behavioral attributes, such as signature, keystroke, voice and gait style. Among these features, iris recognition is one of the most attractive approaches due to its nature of randomness, texture stability over a life time, high entropy density and non-invasive acquisition. While the performance of iris recognition on high quality image is well investigated, not too many studies addressed that how iris recognition performs subject to non-ideal image data, especially when the data is acquired in challenging conditions, such as long working distance, dynamical movement of subjects, uncontrolled illumination conditions and so on.

There are three main contributions in this paper. Firstly, the optical system parameters, such as magnification and field of view, was optimally designed through the first-order optics. Secondly, the irradiance constraints was derived by optical conservation theorem. Through the relationship between the subject and the detector, we could estimate the limitation of working distance when the camera lens and CCD sensor were known. The working distance is set to 3m in our system with pupil diameter 86mm and CCD irradiance 0.3mW/cm^2. Finally, We employed a hybrid scheme combining eye tracking with pan and tilt system, wavefront coding technology, filter optimization and post signal recognition to implement a robust iris recognition system in dynamic operation. The blurred image was restored to ensure recognition accuracy over 3m working distance with 400mm focal length and aperture F/6.3 optics. The simulation result as well as experiment validates the proposed code apertured imaging system, where the imaging volume was 2.57 times extended over the traditional optics, while keeping sufficient recognition accuracy.

Key words: unconstrained iris recognition, extended depth of field, image restoration

1. Introduction

Using biometric features for identity recognition has been practiced for centuries. Basically, the personal attributes used for a biometric identification system can be classified into two categories: the first one is based on physiological attributes, such as DNA, facial features, retinal vasculature, fingerprint, palm print, hand geometry and iris texture; the other one is dependent on behavioral attributes, like signature, keystroke, voice and gait style [1]. In many applications, biometrics recognition has become a key technology for identity management systems. Among these features, iris recognition is the most attractive one due to its nature of random and stable texture, high entropy density and noninvasive assessment.

The iris is an annular membrane between pupil and sclera in the eye. According to Daugman's algorithm, the probability of false identification is of the order of 10^{-10} [2-4], which means the probability is smaller than 1 by two iris codes have the same each other in the world. Iris recognition system consists of three major parts, as shown in Figure 1:

I. Iris image acquisition,

II. Iris image processing, and

III. Feature matching.

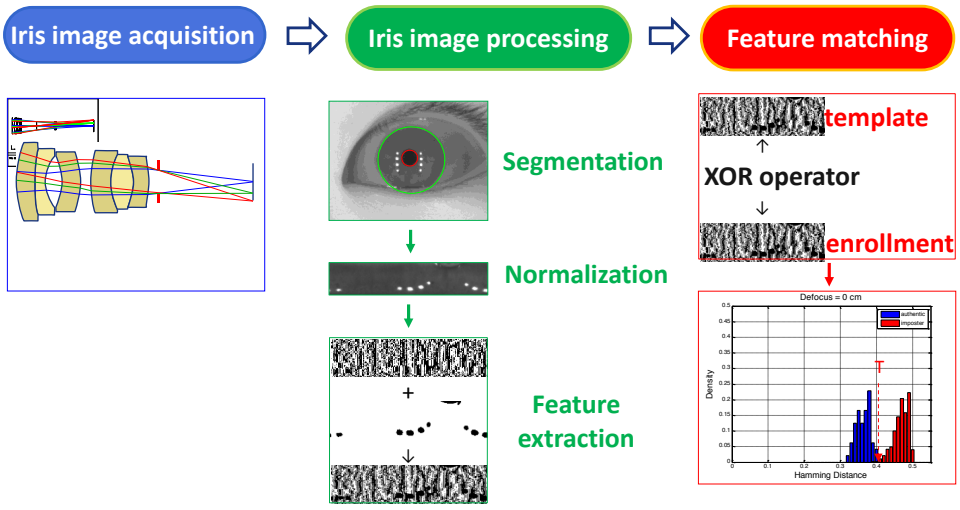

Figure 1. Flowchart of iris recognition system.

Recently, high-speed iris capturing devices have become available on the market. These devices are capable of capturing iris images of both eyes in less than three seconds per person. One example of a high-speed system is the Iris-On-the-Move (IOM) system, manufactured by Sarnoff Corporation [5]. IOM has the capability of taking a video of subjects as they are walking through the portal. The subjects do not need to stop at any point during the acquisition process. All he/she has to do is to walk through the portal while looking straight ahead. The cameras inside the cabinet will automatically capture the iris images.

For such long distance iris acquisition device, DoF of the system is the higher and better in order to allow maximal

mobility of the subjects. In this work, we employed the technique of optical phase modulation [6-9] to increase DoF of a less constrained iris acquisition system. Experimental results show that the proposed scheme can successfully triple the DoF.

2. Optical system parameter setup

2.1. Field of view and resolution

The major challenge in current long range iris acquisition system lies in these two fundamental constraints: the first one is the resolution limitation of the sensor. According to the ISO/IEC 19794-6, the resolution across the iris region should be larger than 150 pixels to ensure the acceptable image quality [10-11]. The specification of the sensor and telephoto lens we used in our experiment are shown in Table 1. From Table 1, it can be calculated that the optical resolution for 1.2 mm on the target object is 150 pixels. Since the width of the iris is about 12mm for an adult [12], such requirement gives a constraint that the magnification of the imaging system has to be larger than 0.1, and corresponding focal length has to be larger than 272 mm.

The other constraint lies in the field of view: size of captured facial image on the sensor should be large enough to cover the entire ocular region which can characterize the periocular feature and enhance the system stability [13]. Our image sensor size is 16.64 mm, which results in the magnification of the imaging system being smaller than 0.1664, corresponding to a 428mm focal length. As shown in Figure 2, in order to meet these two requirements on focal length (the orange slash area), we select a commercial available telephoto zoom lens, whose specification is shown in Table 1. The working distance of the proposed system ranges from 220 cm to infinity with adjustable focal length from 150 to 500 mm. Here we set our operation focal length about 400 mm.

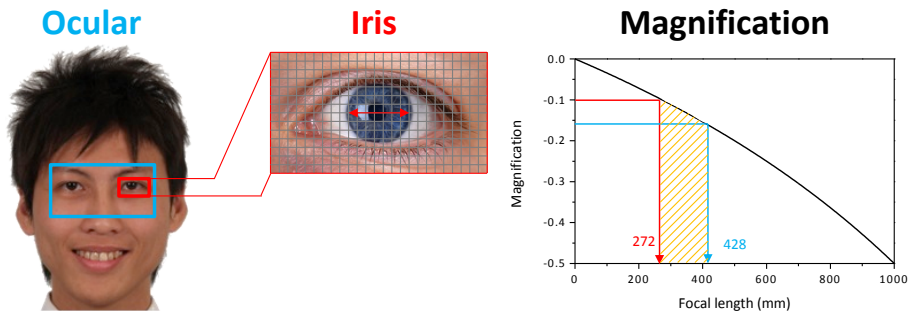

Figure 2. Optical consideration in long distance (3 meter) iris acquisition.

Table 1. Specification of sensor and telephoto lens.

MV1-D2080 IR CCD		**Sigma APO 150-500 mm**	
Optical format	23.5 mm	Field of View	16-5 deg
Resolution	2080×2080	Minimum Distance	220 cm
Pixel Size	8μm	Maximum Magnification	1 : 5.2

Dark current	0.65 fA/pixel	Caliber Diameter	86 mm

2.2. Depth of field

Depth of Field (DoF) of an optical system is the distance between the nearest and farthest position that an object appears as a sharp image on the photo sensor. DoF is dependent on the objective distance, focal length, entrance pupil and circle-of-confusion (CoC). Figure 3 schematically illustrates the concept of DoF (orange slash area), where s_o , s_i and f represent the object distance, image distance, and focal length, respectively. When the subject is located in front or behind the object plane, it causes blur spot on the image plane. Here we use variable c to represent the size of CoC as the maximally allowable blurred spot in the recognition process. Let D_n and D_f represent the near and far limits of DoF respectively. The subject located in front or behind the object plane can be described by equation (1) and (2), where a denotes the entrance pupil diameter.

$$\frac{1}{s_i\left(1+c/\left(a-c\right)\right)}-\frac{1}{s_o-D_f}=\frac{1}{f} \tag{1}$$

$$\frac{1}{s_i\left(1-c/\left(a+c\right)\right)}-\frac{1}{s_o+D_f}=\frac{1}{f} \tag{2}$$

D_n and D_f can be defined by equation (1) and (2):

$$D_n=\frac{-cs_o\left(f+s_o\right)}{fa-c\left(f+s_o\right)} \tag{3}$$

$$D_f=\frac{-cs_o\left(f+s_o\right)}{fa+c\left(f+s_o\right)} \tag{4}$$

It should be noted the CoC can be defined differently according to the purpose of the designed optical system. Traditional CoC depends on visual acuity, but in this paper CoC is defined as the size of the Gaussian which is used to convolve with the original iris image. As long as the iris image, after convolved with the Gaussian, can be successfully matched to its clear version, such level of CoC is acceptable in terms of the required accuracy of iris recognition. Through the simulation, the allowable size of CoC is 0.136mm.

Here we set our CoC as 0.136 mm, the focal length as 400 mm and subject distance as 3000 mm of the iris capturing system. The pupil size approximates 86 mm of caliber diameter. The corresponding DoF, after calculation, is about 60 mm. The range is really tight for typical iris acquisition, especially for long-range system. The purpose of our work is to provide an optical method for extending the DoF of long distance iris recognition system.

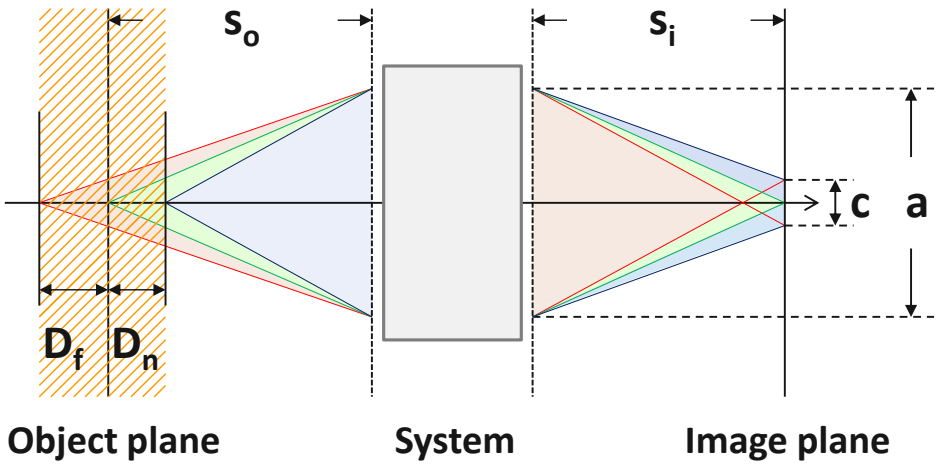

Figure 3. The schematic diagram for depth-of-field formulas.

2.3. Optical phase modulation

In order to extend the DoF, we utilized an optical phase modulation technique called wavefront coding technology. Unlike the conventional imaging system whose point spread function deteriorates due to the defocus, we place a coded phase mask on the pupil plane to engineer the point spread function insensitive to the defocus. The modified point spread function exhibits a triangle distribution over a certain working distance. With appropriate image post-processing technique such as Wiener filter, we can restore the intermediate image to adequate fidelity. The restored iris images can be used for recognition purpose in later stages. The phase profile is given by [6]

$$P(x,y) = \exp\left[i\alpha\left(x^3 + y^3\right)\right] \tag{5}$$

where $P(x, y)$ is the pupil function and the indices x and y are normalized coordinates in the pupil plane. Furthermore, the choice of α governs the overall strength of the mask. In other words, larger α causes high invariance but decreases modulation transfer function values. In order to design the profile with appropriate α value, we should carefully balance the tradeoff between modulation transfer function of the coded image and desired extended DoF range. The optimal α value obtained in our system is approximately 42 .

2.4. Illumination

In order to validate the proposed methodology, we setup a near-IR iris acquisition system with extended DoF technology. As shown in Figure 4, the subject is walking through a gate, and both sides of the gate are equipped with near-IR LED arrays for environmental illumination. The iris images captured under near-IR wavelength reveal the most discriminative details of iris patterns for the purpose of iris recognition. With wavefront coding and optimized filter design, we can extend the original DoF from about 60 mm to 200 mm, which is around three times larger than the original one. This is a

huge improvement in iris image acquisition technology considering the fact that DoF of current long-range recognition system is about 50-120mm [5].

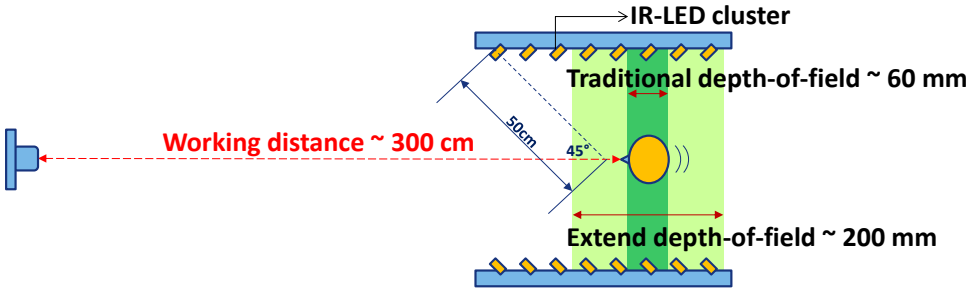

Figure 4. Illustration of the proposed 3m iris acquisition system with LED on both sides. The light sources are commercial infrared LEDs with intensity 2000mW/sr.

In additional to the imaging system, the irradiance consideration is another big issue, which influences the image quality in certain level. In this case, we equip total 96 LEDs on both sides of the gate to keep sufficient irradiance on the subjects' faces. In general, the irradiance is the higher the better, but the minimal irradiance for acceptable SNR should be larger than 30 mW/cm^2. On the other hand, the irradiance should not exceed ICNIRP rule whose IR safety guide for max irradiance about 100 mW/cm^2 [14]. The adequate geometric layout and first-order optical design is used to offer the uniform irradiance as well.

3. Experiment

To measure the point spread function (PSF) of the proposed system, we used a point source at different positions of the object plane. The results are shown in Figure 5. The first row and the second row is the measured result when the system is without and with cubic phase mask, respectively. The sub-figure from left to right shows variant PSFs when the defocus distance ranges from -15 cm to +15 cm. The geometrical size and energy distribution of the PSFs in the first row are varying with different levels of defocus while the PSFs in the second row keep almost the same. In other words, the cubic phase mask makes the PSF insensitive to defocus.

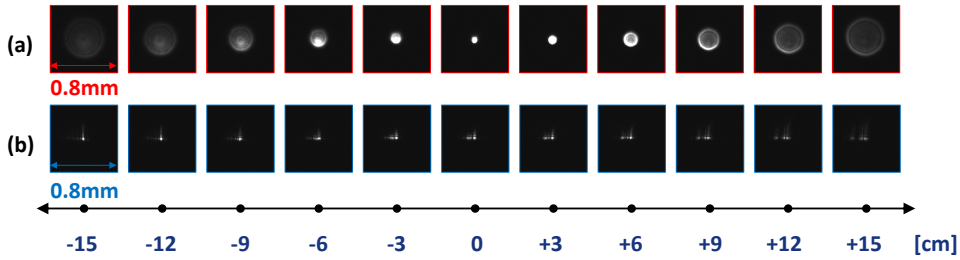

Figure 5. (a) The point spread function without modulation by cubic phase mask (b) The point spread function with modulation by cubic phase mask .

Captured images without, with extended DoF, and extended DoF with Wiener filter are shown in Figure 6 (a), (b) and (c), respectively. After comparing them, we can see that the wavefront coding technique enables the image blur less sensitive to the defocus effect. The optimal operating range is about -3.42 cm to 12 cm. Beyond such limit, the triangular point spread function is too large and the captured image cannot be recovered to the acceptable quality for the purpose of recognition.

The experiment collects 12 subjects and each one has 8 pictures of enrollment, each person has 2 rounds and 11 pictures of different defocus. In this paper, experimental results has combined three selective methods into four parts, including without cubic phase mask case, with cubic phase mask and restoration with Wiener filter case and two cases with super resolution algorithm.

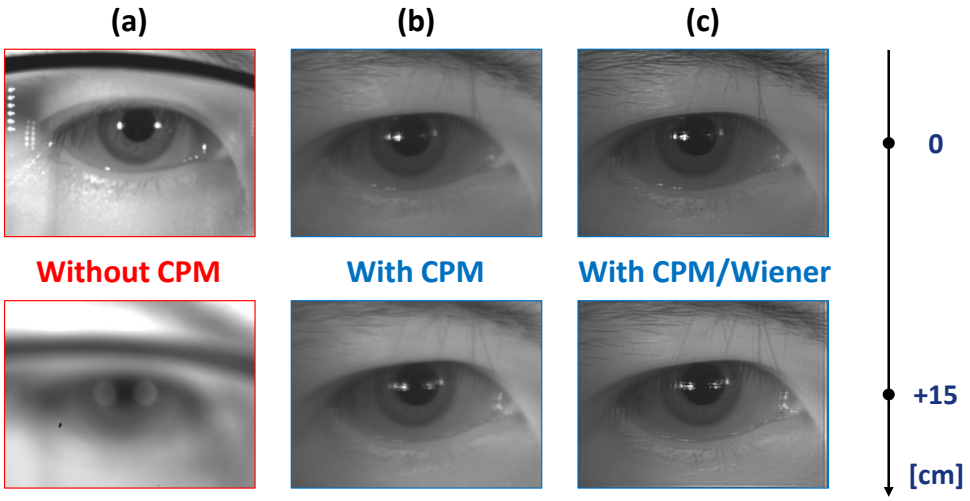

Figure 6. (a) The iris image without modulation by cubic phase mask (b) The iris restored image by Wiener filter.

Performance estimation of iris recognition is done by measuring false acceptance rate (FAR), false rejection rate (FRR) and error equal rate (EER). FAR is the ratio of false acceptance number to total test number. FRR is the ratio of false rejection number to total test number. EER is the value of FAR when it is equivalent to FRR. In addition, we also measured the Fisher ratio. Fisher ratio is the metric describing the distance between two classes distributions.

3.1. Performance of iris recognition without cubic phase mask

Figure 7 (a) shows the authentic and impostor Hamming distance (HD) histogram distribution without cubic phase mask when it is onfocus. Fisher ratio is 2.509; FRR=0.521% when FAR=0.1%; FRR=1.042% when FAR=0%; and EER=0.521%. Under onfocus condition, we found that HD=0.411 when FAR=0.1%. We use such HD as adapted threshold for later experiments. Figure 7 (b) shows authentic and impostor HD distribution versus various defocus range when the HD is set to 0.42. Blue and Red square dot markers denote the authentic and impostor experimental data, respectively. Authentic test is rapidly increase when increase defocus length. Black circle dot markers represent the FRR value. We can see the more defocus the higher FRR is. According to the optical definition from section 2.2, the definition of original DoF is 60mm (orange area). Therefore, we take the value 18.75% as the FRR tolerant boundary.

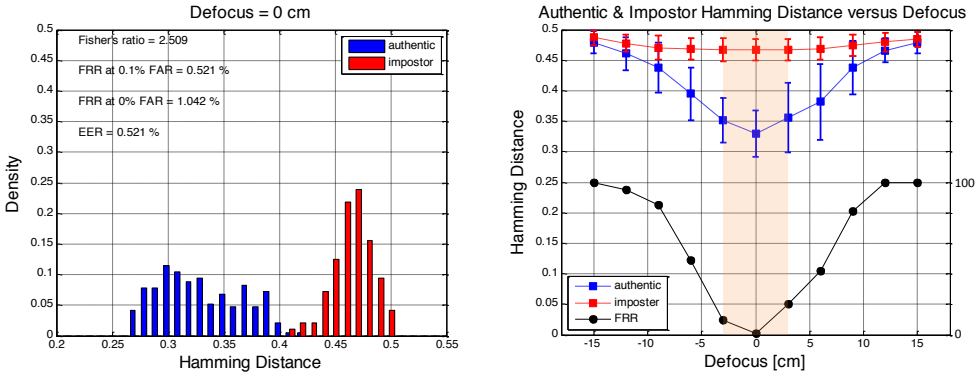

Figure 7. (a) HD histogram distribution of authentic/impostor iris matching without cubic phase mask on focus. (b) HD histogram distribution of authentic/impostor iris matching without cubic phase mask at different defocus distance.

3.2. Performance of iris recognition with cubic phase mask

Figure 8 (a) shows the authentic and impostor HD histogram distribution with cubic phase mask when onfocus. Fisher ratio is 2.124; FRR=0.083% when FAR=0.1%; FRR=0.104% when FAR=0%; and EER=0.083%. Under onfocus condition, we found that HD=0.403 when FAR=0.1%. We use such HD as adapted threshold for later experiments. Figure 8 (b) shows authentic and impostor HD distribution versus various defocus range when HD is set to 0.403. HDs of authentic comparison are slowly increasing when the iris is positioned further defocus. Black circle dot markers represent the FRR value. Comparing to the case without cubic phase mask, FRRs are increasing less rapidly when increasing defocus range. According to the tolerant boundary defined from section 3.1, the acceptable FRR is 18.75%. Therefore, we take the value FRR=18.75% as a threshold. We claim that iris images are clear enough if FRR does not exceed such threshold. Under such condition, the DoF is extended to 2.57 times compared to the original system (without cubic phase mask).

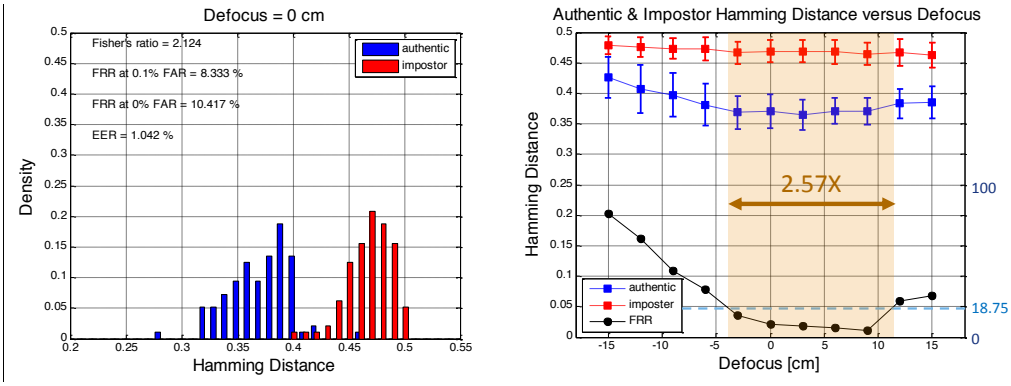

Figure 8. (a) HD histogram distribution of authentic/impostor iris matching with cubic phase mask on focus. (b) HD histogram distribution of authentic/impostor iris matching with cubic phase mask on different defocus.

3.3. Performance of iris recognition without cubic phase mask/with super resolution

In this sub-section, we would like to incorporate image super-resolution (SR) technique into our framework. SR is an image processing technique to estimate high resolution images from low resolution ones. It was also widely used as

means to restore blur and noisy image back to its clear version. We propose to use SR technique in the proposed EDoF system to enhance the quality of the iris image acquired by our system. There are many existing image SR algorithms. The one we used in the experiment was proposed by Nguyen et al. [15], which is particularly designed for restoring the iris images for less constrained environment and on the move.

In order to fairly measure the performance of the SR, we perform SR on (1) original system (without cubic phase mask) and (2) the proposed EDoF system (with cubic phase mask). The results are presented as plots of HD distribution of both authentic and imposter comparison. They are shown in Figure 9 (a) (for original system) and (b) (for EDoF system).

From Figure 9 (a), we can see that without using cubic phase mask (the original system), SR does not bring advantages to the original system. The two distribution intersects with each other, meaning that the iris images after performing SR are still very blur. The image quality is not improved to a recognizable level. On the other hand, in Figure 9 (b) we see a completely different result. The two distribution separate from each other, meaning SR technique did enhance the quality of iris images and improve the overall recognition rate. Therefore, we conclude the proposed cubic phase mask system combined with image SR technique works pretty well as a long-range iris acquisition system. Such design greatly extends the depth-of-field of the original system, at the same time, it also maintains the recognition performance.

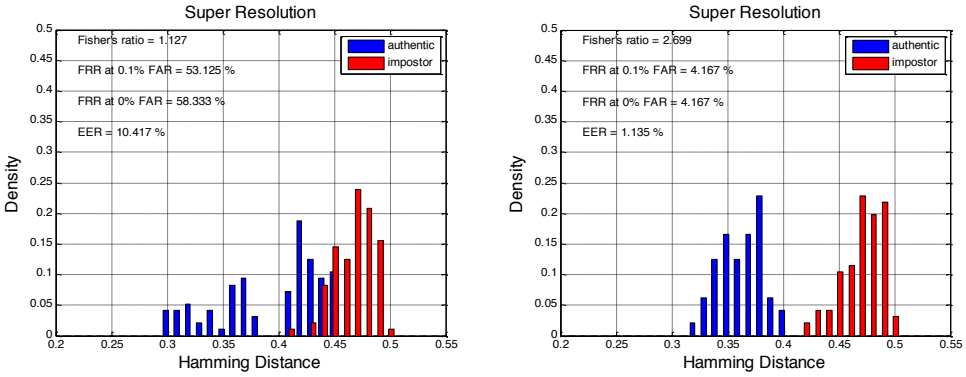

Figure 9. HD histogram distribution of authentic/impostor iris matching after performing image super-resolution (a) in the original system. The two distribution intersects, which means the SR technique does not work well for the original system (b) in the EDoF system. The two distribution separate from each other, which means SR technique improves system accuracy for the proposed system.

Conclusions

Extending DoF with optical phase modulation is a very useful technique to enhance the usability for image acquisition devices. In this study, we implemented a telephoto imaging system to acquire iris images from three meters away, which is practically useful for many applications which require high turnover rate. The computational imaging scheme can greatly increases the DoF to be approximately three times the conventional imaging system, while keeping sufficient recognition accuracy. Future work includes synchronizing the camera system with continuous shooting function for better convenience for long-range iris image acquisition.

Acknowledgement

This work was supported by National Science Council of Taiwan under contract no. NSC-101-2221-E-035-084 and 101-2221-E-009-113.

Reference

[1] A. K. Jain, A. Ross, and S. Prabhakar, "An Introduction to Biometric Recognition," IEEE Transactions on Circuits and System for Video Technology, 14(1), 4-20 (2004).

[2] J. Daugman, "The importance of being random: statistical principles of iris recognition," Pattern Recognition 36, 279-291 (2003)

[3] J. Daugman, "High confidence visual recognition of persons by a test of statistical independence," IEEE Transaction on Pattern Analysis and Machine Intelligence 15(11), 1148-1161, (1993)

[4] J. Daugman, "How iris recognition works," IEEE Transaction on Circuits and Systems for Video Technology 14(1), 21-30 (2004)

[5] J. R. Matey, O. Naroditsky, K. Hanna, R. Kolczynski, D. J. Lolacono, S. Mangru, M. Tinker, T. M. Zappia, and W. Y. Y. Zhao, "Iris on the Move: Acquisition of Images for Iris Recognition in Less Constrained Environments," Proceedings of the IEEE 94(11), 1936-1947 (2006)

[6] E. R. Dowski, and W. T. Cathey, "Extended depth of field through wavefront coding," Applied Optics 34(11), 1859-1866 (1995)

[7] S. Sherif, E. Dowski, and W. Cathey, "A logarithmic phase filter to extend the depth of field of incoherent hybrid imaging systems," Algorithms and Systems for Optical Information Processing V, 272-279 (2001)

[8] K. Kubala, E. Dowski, J. Kobus, and R. Brown, "Design and optimization of aberration and error invariant space telescope systems," Proceeding of the SPIE 5542, 54-65 (2004)

[9] Z. Zalevsky, "Extended depth of focus imaging: a review," SPIE Rev. 1, 012001 (2010)

[10] ISO/IEC 19794-6:2005, "Information technology - Biometric data interchange formats - Part 6: Iris image data"

[11] ANSI INCITS 379-2004: Iris Image Interchange Format

[12] J. V. Forrester, A. D. Dick, P. G. McMenamin, and W. Lee, [The eye: basic sciences in practice], 2nd ed. (W.B. Saunders, London, 2001)

[13] U. Park, A. Ross, and A. K. Jain, "Periocular biometrics in the visible spectrum: A feasibility study." To appear in Biometrics: Theory, Applications and Systems (2009)

[14] D. Sliney, D. Aron-Rosa, F. DeLori, F. Fankhauser, R. Landry, M. Mainster, J. Marshall, B. Rassow, B. Stuck, S. Trokel, T. M. West, and M. Wolffe, "Adjustment of guidelines for exposure of the eye to optical radiation from ocular instruments: statement from a task group of the International Commission on Non-Ionizing Radiation Protection (ICNIRP)," Applied Optics 44(11), 2162-2176 (2005)

[15] K. Nguyen, C. Fookes, S. Sridharan, S. Denman, "Quality-Driven Super-Resolution for Less Constrained Iris Recognition at a Distance and on the Move," IEEE Transactions on Information Forensics and Security 6(4), 1248-1258(2011)